

# Self-Sensing Pneumatic Artificial Muscle with Unilateral Expansion and High Contraction Ratio for Wearable Robotics

Jian Li<sup>1</sup>, Mengqian Tian<sup>2</sup> and Xingsong Wang<sup>1+</sup>

<sup>1</sup> School of Mechanical Engineering, Southeast University

**Abstract.** Pneumatic artificial muscles is widely used in robots and rehabilitation devices, but it is difficult to achieve both high contraction ratio and wearing comfort. In order to solve this problem, we propose a kind of pneumatic artificial muscle with unilateral expansion and high contraction ratio (UEPAM). The UEPAM is composed of a bending layer, several folding balloons, and 3D printed flatbeds, which can be fabricated simply by laser cutting and 3D printing. The static experimental results show that the maximum shrinkage of UEPAM can reach 69% under 15N load. The dynamic experimental results show that the artificial muscle has good position tracking ability for 0.5Hz sinusoidal signal with the maximum displacement error of 1.2 cm when closed-loop control is adopted. More importantly, due to the limitation of 3D printing rigid parts, UEPAM can only expand on one side during inflation, which makes it more suitable to be arranged in soft wearable devices without squeezing the wearer's skin. In addition, we integrate a resistive sensor based on bending measurement to sense shrinkage and displacement by measuring the bending degree of the actuator's bending layer. The experimental results show that the sensor has good accuracy and repeatability.

**Keywords:** pneumatic artificial muscle, soft wearable devices, unilateral expansion, measurement.

## 1. Introduction

Pneumatic artificial muscles have been widely used in various robotic and rehabilitation medical devices in recent years [1]-[4]. Compared with the traditional rigid actuator, pneumatic artificial muscle has simple structure and light weight. At the same time, it has higher safety in man-machine contact because of its good compliance [5]. These characteristics of pneumatic artificial muscle make it have a great application prospect in flexible wearable devices.

The earliest pneumatic artificial muscles can be traced back to the McKibben inflatable muscles designed by American doctor McKibben in 1960s, which was used to drive artificial limbs [6]. The internal structure of McKibben artificial muscle is a rubber tube, and the outer surface of the rubber tube is wrapped with a double helix fiber braid. When it works, the rubber tube will expand radially, the pneumatic muscle will contract axially because of the rigidity of the outer braid, resulting in pulling force to drive the load. However, due to the restriction of knitting structure, the contraction of McKibben artificial muscle is relatively small (30 ~ 35%) [7].

With the continuous innovation and improvement of researchers, there are more and more kinds of pneumatic artificial muscles, including braided type [8],[9], wrinkled type [10]-[13] and curved type [14]-[17]. These pneumatic artificial muscles were optimized in weaving methods and fabrication materials, which improve the contraction performance of artificial muscles. The "18 Weave" Muscles utilized the flexibility of the thin McKibben muscle to achieve 19.4% additional displacement. The pleated PAM has a larger stroke and is less affected by friction related hysteresis. Curved artificial muscles are composed of molded elastomer cavities and fiber-reinforced materials that produce specific bending, twisting, and extension trajectories under fluid compression. Although these artificial muscles are more abundantly diverse in geometry, contraction mode, and fabrication materials, they cannot effectively increase the contraction ratio and output force.

Bellows textile muscle works by providing negative pressure to the chamber, which flattens to bring artificial muscle contraction [18]. The contraction ratio of this artificial muscle can be very large. Origami

---

<sup>+</sup> Corresponding author. Tel.: + 8613951905660.  
E-mail address: 101003909@seu.edu.cn.

vacuum pneumatic artificial muscle has an origami structure and can achieve a 62% shrinkage rate [19]. These artificial muscles rely on internal and external pressure differences to produce deformation and are suitable for applications where small forces are required. HCRPAM [20] can shrink greatly and produce a larger force, with a shrinkage ratio of 64.7%, but it is bulky, incompact and may bend when inflated, which is not good for wear.

In addition, some artificial muscles are designed with embedded sensors to facilitate measurement and precise control. The ultrasonic sensor installed in the rubber artificial muscle can be used as a displacement sensor [21]. Experiments show that the measurement error of artificial muscle position can be reduced by arranging light reflectors in the radial direction [22].

To solve the problem of high contraction ratio and wearable performance of artificial muscles, in this paper, we propose a pneumatic artificial muscle with unilateral expansion and high contraction ratio. The UEPAM is composed of a bending layer, multiple folding balloons, and 3D printed flatbeds. By combining the bending layer and several folding balloons by simple weaving, the lateral expansion of folding balloons makes the artificial muscle contract vertically, and the contraction rate is significantly higher than that of the traditional McKibben pneumatic artificial muscle. In addition, the 3D printing part limits one side of the folded balloons, so that the balloons can only expand to the other side without squeezing the other side, making the artificial muscle more suitable to be arranged on the wearable device.

Furthermore, it integrates a resistance bending sensor, which can sense the displacement of artificial muscle by measuring the curvature of bending layer. The self-sensing sensor makes use of the relationship between the contraction rate of the artificial muscle and the curvature of the bending layer, and obtains the real-time displacement of the artificial muscle without affecting the work of the actuator, which is more conducive to closed-loop control.

## 2. Method

### 2.1. Structural Design

As shown in Fig. 1 and Fig. 2, the UEPAM is composed of a bending layer, multiple folding balloons, 3D printed flatbeds, and bending sensor clinging to the bending layer. Two strip grooves with rounded corners are designed at both ends of the 3D printing plates, so that the bending layer can pass through smoothly. The folding balloons are composed of several flat balloons in series and are arranged between the bending layer and the 3D printing plate. When not inflated, the thickness of the folded balloons is approximately zero and the overall structure is compact.

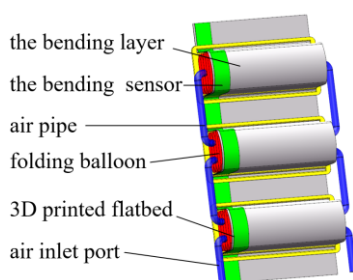


Fig. 1: Structure of the UEPAM.

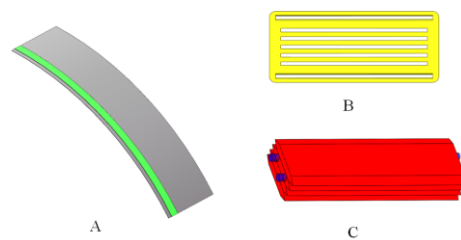


Fig. 2: Components of the UEPAM. (A) the bending layer with sensor; (B) 3D printed flatbed; (C) folding balloon.

As shown in Fig. 3, when the balloons are inflated, the folded flat balloons expand along the thickness direction. Due to the limitation of 3D printing rigid plate, the balloons expand only to one side. At the same time, the folding balloons will stretch out the curved layer, which limits its expansion. The curvature of the curved layer increases, causing the artificial muscle to contract along the length, along with a shorter distance between the two ends. The bending layer is made of thin film material with high tensile strength and low bending stiffness. It can be considered that the length of the bending layer does not change during the bending process, therefore, an increase in the curvature of the curved layer can lead to a shorter distance

between the two ends of the artificial muscle. The curvature variation can be accurately measured by a bending sensor attached to the bending layer. The folding balloons is made of inelastic material, which can ensure the structural stability of the artificial muscle when it is working.

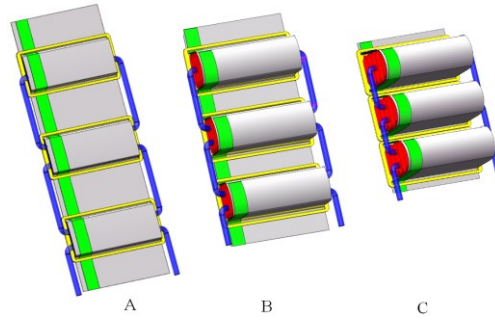


Fig. 3: The UEPAAM under different air pressures (A) Uninflated state; (B) Semi-inflatable state; (C) Fully inflatable state.

In addition, several folding balloons can be attached on a curved layer by weaving, and the folding balloons are connected through the soft tubes, which effectively increases the contraction ratio and output force of artificial muscles while guaranteeing a compact structure.

## 2.2. Modelling

### (1) Artificial muscle modeling

In order to determine the quantitative relationship between the parameters of the artificial muscle and the contraction rate, it is necessary to model and analyze the artificial muscle. The following assumptions are made to simplify the analysis: 1) The material of the balloons is inelastic, and the cross-sectional perimeter of a single balloons remains the same all the time. 2) The cross section of a single small balloons in a folded balloons is symmetrical when inflated, which can be assumed to be a diamond. 3) Each small balloons in the folded balloons expands equally.

In the inflated state, the force analysis of the basic unit of the artificial muscle is shown in Fig. 4.

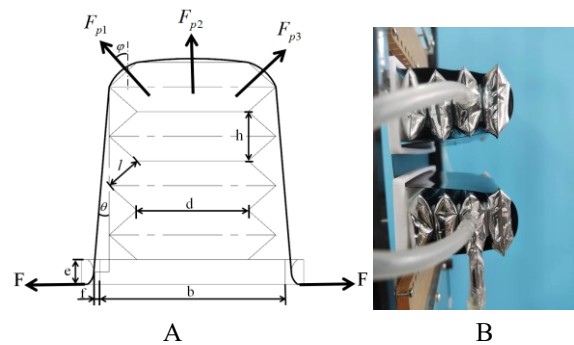


Fig. 4: The basic unit of UEPAAM. (A) The force analysis of model; (B) The actual unit.

Suppose that in the initial state, the number of small balloons inside the folded balloons is  $m$ , the length is  $a$ , the width is  $b$ , the rectangle used for the bonding of the two small balloons is  $c$ , the width is  $d$ . After inflation, the height of a single balloons is  $h$ . The length of the bevel of the diamond section  $l$  can be calculated by (1).

$$l = (b - d) / 2 \quad (1)$$

The load force at both ends of the artificial muscle  $F$  and the balloons drive force  $F_p$  form a three-force balance. The relationship can be described by (2).

$$F_p = 2F \cos \theta \quad (2)$$

In the formula,  $\theta$  is the angle between the bending layer on the sides of the balloons and the expansion direction of the balloons, which can be calculated by (3).

$$\cos \theta = \frac{(m - \frac{1}{2})h + \frac{e}{2}}{\sqrt{[(m - \frac{1}{2})h + \frac{e}{2}]^2 + (\frac{b}{2} - \frac{d}{2} - \sqrt{l^2 - (\frac{h}{2})^2 + f})^2}} \quad (3)$$

The balloons' drive force  $F_p$  is divided into three parts as show in (4)-(6).

$$F_p = F_{p1} + F_{p2} + F_{p3} \quad (4)$$

$$F_{p2} = k_1 pad \quad (5)$$

$$F_{p1} = F_{p3} = k_2 pal \cos \varphi \quad (6)$$

$\varphi$  can be calculated by (7).

$$\cos \varphi = \frac{\sqrt{l^2 - (\frac{h}{2})^2}}{l} \quad (7)$$

Thus, the contraction displacement of the artificial muscle  $\Delta x$  can be calculated by (8).

$$\Delta x = \frac{2(m - \frac{1}{2})}{\cos \theta} h \quad (8)$$

The contraction rate of artificial muscle  $\varepsilon$  can be calculated by (9).

$$\varepsilon = \frac{2k_3(m - \frac{1}{2})}{l_0 \cos \theta} h \quad (9)$$

Where  $k_3$  is the number of folded balloons and  $l_0$  is the initial length of the artificial muscle.

## (2) Bending sensor modeling

In the process of artificial muscle contraction, with the increase of contraction displacement, the proportion of the bending part in the bending sensor to the total length becomes larger. Also, with the increase of  $\cos \theta$ , the degree of bending becomes larger. Therefore, the preliminary modeling of the bending sensor is as (10).

$$\lambda = k_b \Delta x \cos \theta \quad (10)$$

Where  $\lambda$  represents the bending degree of the bending sensor.

## (3) Fabrication

The UEPAM is composed of a bending layer, multiple folding balloons, 3D printed flatbeds, and the bending sensor clinging to the bending layer.

- **Bending layer:** According to the previous analysis, the bending layer should have the characteristics of easy bending and non-stretching, and the friction coefficient of the material should be as small as possible to ensure the fluency of the artificial muscle during contraction. PET materials have both good tensile and bending properties, and the surface is smooth, so we chose pet to make the bending layer. The PET layer can be conveniently and quickly cut into designed shapes by a laser cutting machine, and then the bending sensors are stuck onto the thin layer curved surface, as shown in Fig. 5(A).
- **Folding balloons:** The inflation performance of the folded balloon plays a crucial role during artificial muscle contraction. In order to ensure the stability and rapidity of balloons expansion, the materials used to make balloons need to meet the requirements such as good gas tightness, pressure resistance, and small surface friction coefficient. Considering the outstanding comprehensive properties of the aluminum-plastic membrane, we chose the aluminum-plastic membrane as the fabrication material for a single air pouch. Aluminum plastic membrane was composed of an aluminum membrane in the middle and pet layers on both sides. The aluminum film in the middle gives it high tensile properties, which guarantees the air tight and pressure resistance properties of the balloons, the pet layer on both

sides has a small surface friction coefficient, which gives it less resistance when the air bag is inflated. When making balloons, firstly two aligned aluminum-plastic films are bonded by a hot press, and which removes the air between the two layers of aluminum-plastic films. Then several balloons are cut out by a laser cutting machine, each of which is glued with double-sided glue. After that a punch is used to punch holes in the folded balloons to connect each balloons. Finally, seal the upper and lower bottom holes and install the air pipe for the fabricated folding balloons. After testing, the balloons made by this process can withstand the pressure of 150kpa. The The finished balloons are shown in Fig. 5(C) and Fig. 5(D).

- 3D printed flatbeds: The rigid plate is made of PLA material by 3D printing process,as shown in Fig. 5(B). The processing method of 3D printing can easily create the shape of the design. PLA material is light and rigid, which very meets the requirements for wearable materials.

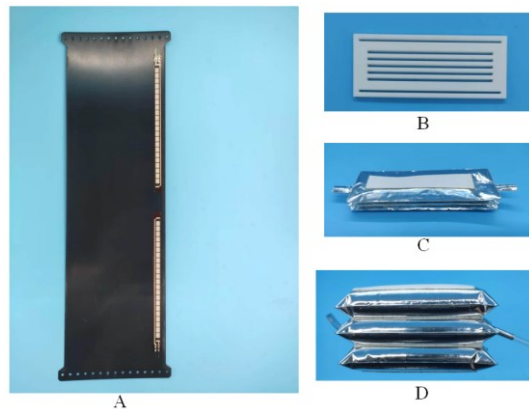


Fig. 5: The components of UEPAM. (A) The bending layer with bending sensor; (B) 3D printed flatbed; (C) Folding balloons (D) Inflatable balloons.

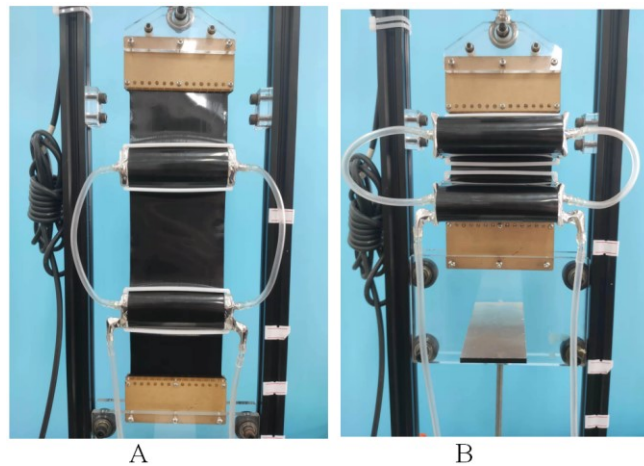


Fig. 6: The finished UEPAM. (A) The UEPAM in the initial state ; (B) The UEPAM in the inflated state.

After the bending layer, folding balloons and rigid plates are fabricated, one side of the folding balloons is fixed on the 3D printing plate, and then the bending layer is alternately passed through the strip groove of the plate. Finally, the folded balloons are connected by soft pipes to complete the production of UEPAM, as shown in Fig. 6. The thickness of the artificial muscle before inflation is only 5mm, and the overall mass is 30g. After the air intake from the lower air inlet, the folding balloons expands, causing the bending of the adjacent bending layer and the contraction of the artificial muscle along the length direction.

### 3. Experiment and Results

#### 3.1. Static Characteristic Experiment

As shown in Fig. 7, the artificial muscle characteristic experiment platform is designed to test the static and dynamic characteristics of UEPAM.

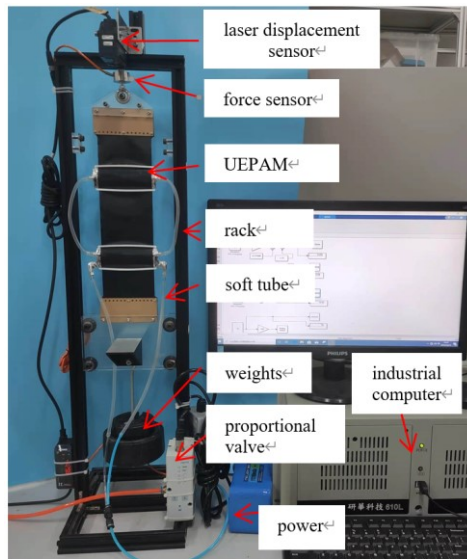


Fig. 7: The artificial muscle characteristic experiment platform.

The platform consists of pneumatic source, pressure reducing valve, sensors, weights and industrial computer. The pneumatic source is XDT550-30L air compressor and the pressure reducing valve is high speed proportional valve (Festo VPPM-6L-L-1-G18-0L6H-V1N). The stable air pressure provided by the air compressor is reduced by the pressure reducing valve and supplied to the artificial muscle. The main sensors are tension sensor (DYM-103) and laser displacement sensor (Keyence IL-1000). The tension sensor measures the output force produced by the artificial muscle under different loads, and the displacement sensor measures the amount of contraction produced by the artificial muscle. After processing the data measured by sensors, the relevant characteristic curves can be obtained and analyzed accordingly.

Under the same inlet pressure, the curve of the relationship between the load value and the shrinkage rate is the isobaric characteristic curve. The isobaric characteristic curve describes the ability of the artificial muscle to hold the load. In the isobaric experiment, there are two folding balloons on the bending layer of the artificial muscle, and each folding balloons is composed of four balloons in series. The experimental pressures are 10kpa, 25kpa, 50kPa and 100kpa respectively. The weights are gradually increased as a load at each fixed pressure until 5.5 kg. The contraction of the artificial muscle was recorded under each group of parameters, and the isobaric curves are shown in Fig. 8.

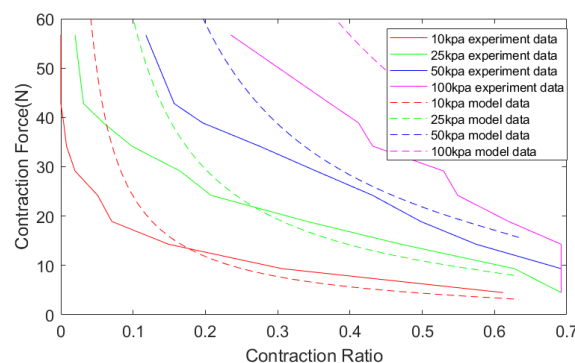


Fig. 8: The isobaric curves and comparison between the model and the experimental.

As can be seen from Fig. 8, the maximum contraction rate of the artificial muscle could reach 69% under the load of 15N. At a contraction rate of 20%, the output of the artificial muscle can reach 55N, which is almost 100 times the mass of UEPAM. When the load is small, the experimental data is close to the model prediction. As the load increases, the contraction force measured in the experiment is smaller than the

theoretical value, which is mainly due to the deflection of the folded balloons. In the future work, we can try to solve this problem by adding rigid constraint in the direction of balloons expansion.

### 3.2. Dynamic Characteristic Experiment

Due to the influence of the compressibility and elasticity of pneumatic artificial muscle, the artificial muscle is nonlinear when it works. Therefore, the tracking effect on sinusoidal signals should be studied here.

#### (1) Sine signal tracking experiment

The industrial computer collects the position information measured by the laser displacement sensor and adjusts the air pressure output under the PID control algorithm. The experimental results are shown in the Fig. 9.

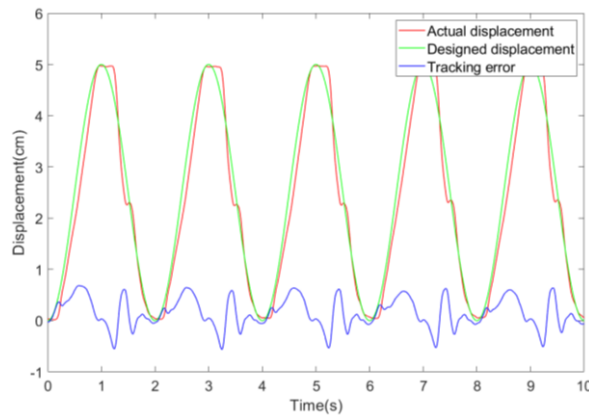


Fig. 9: The experimental results of sinusoidal position tracking.

As shown in Fig. 9, the UEPAM has a good tracking accuracy at a frequency of 0.5 Hz with a maximum error of 1.2 cm.

#### ?? Bending sensor experiment

During the sine tracking experiment, the voltage curve of the bending resistance sensor is obtained as shown in Fig. 10, so that the displacement can be calibrated. The displacement curve converted by the bending Sensor is shown in Fig. 11.

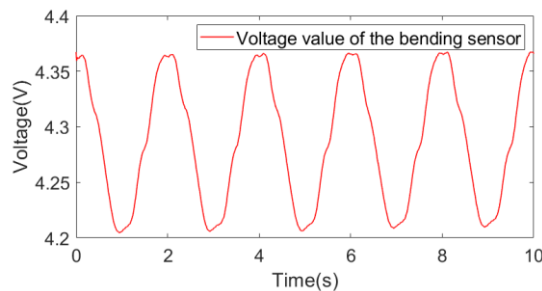


Fig. 10: The voltage-time curve of the bending sensor.

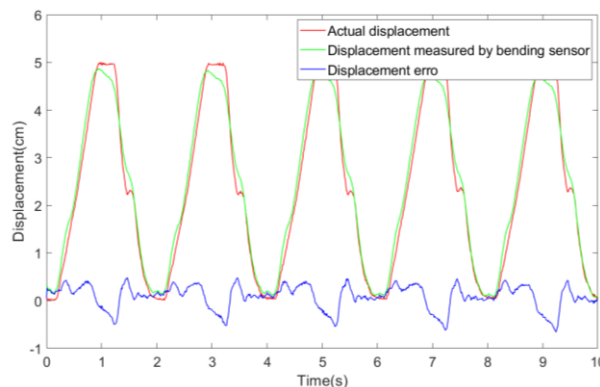


Fig. 11: The Comparison between the displacement measured by the bending sensor and the actual displacement.

The experimental results show that the sensor has good accuracy and repeatability. As can be seen from the diagram, the measuring error of the bending sensor to the displacement is less than 1cm.

#### 4. Conclusion and Future Works

This paper proposed a artificial muscles with unilateral expansion and high contraction ratio(UEPAM). UEPAM is limited by the 3D printed rigid part on one side of the balloons, so that it can only be inflated on one side during inflation, which makes it more suitable to be arranged in soft wearable devices without squeezing the wearer's skin. By combining the bending layer and several folding balloons by simple weaving, the lateral expansion of folding balloons makes the artificial muscle contract vertically, which not only achieves a compact structure but also effectively increases the contraction ratio of the artificial muscle. Experiments show that the maximum contraction ratio of UEPAM is 69%. Of course, the shrinkage of UEPAM can be further improved by changing the parameters of the folding airbag. However, this can make the artificial muscles bulky.

In addition, UEPAM integrates a resistance bending sensor, which can sense the displacement of artificial muscle by measuring the curvature of bending layer. The self-sensing sensor makes use of the relationship between the contraction rate of the artificial muscle and the curvature of the bending layer, which can feedback its contraction state without the expensive external sensors. The experimental results show that the self-sensing sensor has high accuracy and the maximum displacement error is less than 1cm.

In the experiment, we also found many points that can be improved on UEPAM. In terms of structure design, the friction between components should be minimized to alleviate the hysteresis effect caused by friction. In terms of control, more advanced nonlinear control algorithms such as ADRC algorithm can be adopted to improve the dynamic performance of artificial muscles. In addition, UEPAM need be further applied to various wearable exoskeletons to test the performance of artificial muscles and the bending sensor, so as to optimize the structure and theoretical model of artificial muscles.

#### 5. References

- [1] Y. -L. Park, J. Santos, K. G. Galloway, E. C. Goldfield and R. J. Wood, "A soft wearable robotic device for active knee motions using flat pneumatic artificial muscles," 2014 IEEE International Conference on Robotics and Automation (ICRA), 2014, pp. 4805-4810, doi: 10.1109/ICRA.2014.6907562.
- [2] J. Jeong et al., "Wrist Assisting Soft Wearable Robot with Stretchable Coolant Vessel integrated SMA Muscle," in IEEE/ASME Transactions on Mechatronics, doi: 10.1109/TMECH.2021.3078472.
- [3] B. Pawlowski, J. Sun, J. Xu, Y. Liu and J. Zhao, "Modeling of Soft Robots Actuated by Twisted-and-Coiled Actuators," in IEEE/ASME Transactions on Mechatronics, vol. 24, no. 1, pp. 5-15, Feb. 2019, doi: 10.1109/TMECH.2018.2873014.
- [4] P. Beyl, M. Van Damme, R. Van Ham, B. Vanderborght and D. Lefeber, "Pleated Pneumatic Artificial Muscle-Based Actuator System as a Torque Source for Compliant Lower Limb Exoskeletons," in IEEE/ASME Transactions on Mechatronics, vol. 19, no. 3, pp. 1046-1056, June 2014, doi: 10.1109/TMECH.2013.2268942.
- [5] Kellaris, N., et al. "Peano-HASEL actuators: Muscle-mimetic, electrohydraulic transducers that linearly contract on activation." *Science Robotics* 3.14(2018): eaar3276.
- [6] J. L. McKibben, "Artificial muscle," *Life*, p. 87 - 88, Mar 1960.
- [7] Yang, H. D., B. T. Greczek, and A. T. Asbeck. "Modeling and Analysis of a High-Displacement Pneumatic Artificial Muscle With Integrated Sensing." *Frontiers in Robotics and AI* 5(2019).
- [8] Al-Ibadi A, Nefti-Meziani S, Davis S T, et al. Novel Design and Position Control Strategy of a Soft Robot Arm[J]. *Robotics*, 2018, 7(4):72.
- [9] T. Abe et al., "Fabrication of "18 Weave" Muscles and Their Application to Soft Power Support Suit for Upper Limbs Using Thin McKibben Muscle," in IEEE Robotics and Automation Letters, vol. 4, no. 3, pp. 2532-2538, July 2019, doi: 10.1109/LRA.2019.2907433.
- [10] Verrelst, Bj?Rn, et al. "The Pneumatic Biped "Lucy" Actuated with Pleated Pneumatic Artificial Muscles." *Autonomous Robots* 18.2(2005):201-213.

- [11] Daerden, Frank, and D. Lefeber. "The Concept and Design of Pleated Pneumatic Artificial Muscles." *International Journal of Fluid Power* 2.3(2001):41-50.
- [12] Björn Verrelst, et al. "Second generation pleated pneumatic artificial muscle and its robotic applications." *Advanced Robotics* 20.7(2006):783-805.
- [13] D. Villegas, M. Van Damme, B. Vanderborght, P. Beyl, and D. Lefeber, "Third-generation pleated pneumatic artificial muscles for robotic applications: Development and comparison with McKibben muscle," *Adv. Robot.*, vol. 26, no. 11 - 12, pp. 1205 - 1227, 2012.
- [14] Polygerinos, Panagiotis, et al. "Soft robotic glove for combined assistance and at-home rehabilitation." *Robotics and Autonomous Systems* 73.C(2014):135-143.
- [15] Zheng, W., et al. "Interaction Forces of Soft Fiber Reinforced Bending Actuators." *Mechatronics, IEEE/ASME Transactions on* 22.2(2017):717-727.
- [16] Bobak, et al. "Soft Robotics: Pneumatic Networks for Soft Robotics that Actuate Rapidly (*Adv. Funct. Mater.* 15/2014)." *Advanced Functional Materials* 24.15(2014):2109-2109.
- [17] Robert, F, Shepherd, et al. *Soft Machines That are Resistant to Puncture and That Self Seal*[J]. *Advanced Materials*, 2013, 25(46):6709-6713.
- [18] Belforte G , Eula G , Ivanov A , et al. *Bellows textile muscle*[J]. *The Journal of the Textile Institute*, 2014, 105(3):356-364.
- [19] Z. Zhang, W. Fan, G. Chen, J. Luo, Q. Lu and H. Wang, "A 3D Printable Origami Vacuum Pneumatic Artificial Muscle with Fast and Powerful Motion," 2021 IEEE 4th International Conference on Soft Robotics(RoboSoft),2021,pp.551-554,doi: 10.1109/RoboSoft51838.2021.9479194.
- [20] Han K , Nam-Ho K , Dongjun S . *A Novel Soft Pneumatic Artificial Muscle with High-Contraction Ratio*[J]. *Soft Robotics*, 2018:soro.2017.0114-.
- [21] So Shimooka, Shujiro Dohta, Tetsuya Akagi, and Yoshinori Moriwake, "Position Control of Rubber Artificial Muscle Using Built-in Ultrasonic Sensor and Quasi-Servo Valve," *International Journal of Mechanical Engineering and Robotics Research*, Vol.4, No. 4, pp. 304-308, October 2015. DOI: 10.18178/ijmerr.4.4.304-308
- [22] So Shimooka, Tetsuya Akagi, Shujiro Dohta, Shinsaku Fujimoto, and Wataru Kobayashi, "Development of Intelligent Rubber Artificial Muscle with Integrated Pneumatic Driving System and Built-in Inner Diameter Sensor" *International Journal of Mechanical Engineering and Robotics Research*, Vol. 9, No. 1, pp. 136-142, January 2020. DOI: 10.18178/ijmerr.9.1.136-142.